



Axial scanning in lensless microscopy to achieve high resolution

Anwar Hussain^{1,2} · Yicheng Li² · Diyi Liu² · Yinxu Bian² · Cuifang Kuang^{2,3} · Xu Liu^{2,3}

Received: 31 August 2018 / Accepted: 27 January 2019 / Published online: 14 February 2019
© Springer-Verlag GmbH Germany, part of Springer Nature 2019

Abstract

The optical system is designed here, to miniaturize the mechanical scanning and number of phase patterns illumination in lensless microscopy. The random phase mask is positioned in vertical column before the sample, which encoded the sample information and resulted into a final image at the sensor plane. To improve the signal to noise ratio and resolution of final image, the axial direction scanning of sample and sensor (SS) is performed while keeping them mutually immovable. This operation gathered the lost information of sample in between the sample and sensor planes. This axial motion of SS is performed with periodic steps, which would help in the reconstruction process during post processing. The final image has resolution of about 4 μm and field of view of 15 mm^2 . There are numerous advantages of such type of techniques, including portability and fast processing of data.

1 Introduction

The lensless microscopy is a modified version of the conventional lens-based microscopy in which lenses are used to magnify the incoming information [1]. The removal of lens makes the system simple and compact, in which the sample is illuminated and diffraction pattern/hologram is recorded on the sensor's chip directly. The real propagation can be expressed by angular spectrum propagator digitally and the image is reconstructed from the recoded information through reconstruction algorithm. The final image has both the wide field of view and high resolution features. The field of view is restricted by the active area of the sensor rather than the lens magnification factor. The two main classes of lensless microscopy are shadow imaging [2, 3] and fluorescence [4, 5] imaging. The sample in shadow imaging is illuminated with coherent light to record an image at the sensor in transmission modality. To eliminate the twin image effect and improve the signal–noise ratio, different additional

experimental techniques have been implemented [6–9]. The pixel size of the sensor is also a key parameter to limit the resolution which is manipulated through different techniques [10, 11], in which the sensor is translated in x – y plane with sub-pixel shift. This would numerically minimize the pixel size less than its physical size. The study of lensless microscopy is extended while using the phase mask pattern before the sample in the existing setup configuration. The random phase mask is inserted into the system to eliminate the twin image effect during the reconstruction process [12, 13]. The random phase mask pattern encoded the sample information and during post processing all the information decoded conversely. In our previous work, we used multi-angles illumination and multiple-phase masks to improve the resolution [14, 15] beyond the classical value. The diffraction limit imposed on the optical system is extended while bringing the higher spatial frequencies into the pass band of the system. These schemes largely involved the mechanical motion to scan the sample from different angles along x -axis and y -axis which included the extra labor. Such type of techniques would also slow down the processing speed due to the acquisition of large numbers of holograms.

Here, in this paper the multi-heights illumination method is instigated to capture 11 holograms with different heights of phase mask from the sample and further 11 images without sample with the repeated heights of phase mask. The holograms within the pre-defined range of heights in regular periodic steps are sequentially captured. The two types of images are subtracted from each other at their corresponding

✉ Xu Liu
liuxu@zju.edu.cn

¹ Quantum Optics Lab, Department of Physics, COMSATS University, Islamabad, Pakistan

² State Key Laboratory of Modern Optical Instrumentation, College of Optical Science and Engineering, Zhejiang University, Hangzhou 310027, China

³ Collaborative Innovation Center of Extreme Optics, Shanxi University, Taiyuan 030006, China

planes, to eliminate the effect of unscattered beam. All the subtracted result are sequentially propagated to the sample plane through angular spectrum method. The final image with improved resolution and large field of view guarantees the success of this method. The multi-heights method would be easy to be converted into commercial equipment, as it excluded the requirement of different phase mask patterns or component of multi-angles illuminations. The defined step scanning along axial direction is executed through highly precise translator.

2 Working principle of technique

The axial scanning technique is premeditated to improve the capacity of lensless microscopy and overcome the shortcomings reported in other lensless microscopic techniques. In this technique, the coherent laser source from Coherent Company of wavelength 635 nm, is used to illuminate the random phase mask. The phase distribution over phase mask is random with defined range of $(0 \sim 2\pi)$, generated in Matlab and assigned to SLM which is called phase mask throughout the manuscript. The phase mask plane is positioned of z_1 (~ 10 cm) distance, from the sample plane to collect the plane waves as shown in Fig. 1. The sample used for this experiment as well as for simulation is USAF 1951 resolution chart, which works in transmission mode and is well suited to minimize the geometry of optical setup. The CMOS sensor from Sony Company having pixel size of $1.4 \mu\text{m}$ and active area of 15 mm^2 is placed at $950 \mu\text{m}$ distance from the sample plane. At the first flash of coherent source, an image

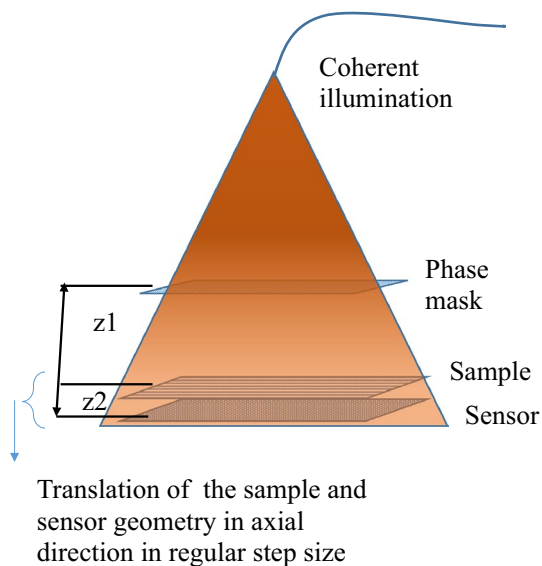


Fig. 1 The experimental setup to perform the axial scanning of the sample and sensor simultaneously along the axial direction

is recorded at the sensor which is back propagated through angular spectrum method to reconstruct the ground truth amplitude and phase of the sample. The retrieved image has very low signal–noise (SNR) ratio and effect of twin image due to two beams interference along the optical axis. These two main complications are resolved through the usage of random phase and axial direction scanning of phase mask. The random phase mask is used in this technique to distribute the twin image effect consistently through the whole sample area. This would minimize the severe twin image effect, which causes the overlap of conjugate image with the real image. The second problem of resolution and SNR improvement, is addressed through the axial scanning of SS. The axial direction motion of SS is controlled through the motorized translation stage KDC101 from Thorlabs, with 25 mm travel range and minimum achievable increment is $0.05 \mu\text{m}$. This would add the precise scanning of phase mask to avoid any error during reconstruction process. The sample and sensor are coupled in a geometry to keep their mutual separation fixed throughout the illumination process. The initial separation of sample from the phase mask is set to be 7.5 cm and then the SS is translated in axial direction in a step size of 0.25 cm. Every time, a hologram is recorded and at the end of the day total of 11 holograms are recorded at each step sequentially which gave the maximum separation z_1 of 10 cm. Similar procedure is followed to record the images without sample which are needed for our algorithm. The travel range of motorized translation stage is 25 mm, which will allow to record large number of hologram while decreasing the step size from 0.25 cm to some lower value. The first image recorded at the CMOS is given in Eq. (1).

$$H = |A + F_r|^2 \quad (1a)$$

The unscattered beam passing through the transparent sample is represented by ' F_r ' and the beam scattered from the sample contents is represented by ' A '. The image recorded without sample in the optical setup is given

$$I = |F_r|^2 \quad (1b)$$

The scattered beam carries the information of plane waves as well as of the sample. To extract the sample information from the recorded hologram, another image without sample is recorded through the same setup, given in Eq. (1b) and subtracted from the hologram Eq. (1a). The random phase mask function is represented in Eq. (1c). At CMOS plane the resultant image is divided with conjugate of phase mask function and propagated to the sample plane. The final operation is the division of image with phase mask function at sample plane given in Eq. (1d). The phase mask function at the sample is represented by ' M_s ', however, 'FSP' represents the free space propagation transfer function.

$$PM = e^{i\varphi(x,y)} \tag{1c}$$

$$M_s = \text{FSP}(e^{i\varphi(x,y)}, z : z_1) \tag{1d}$$

$$O(x, y) = \frac{\text{SF}((H - I)e^{-i\varphi_r t})}{M_s} \tag{2}$$

Equation (2) is construed for single image with fixed z_1 -value. The generalized relation for the range of z_1 -values, is given in Eq. (3), which shows the summation of all retrieved images for post processing.

$$O(x, y) = \sum_{k=1}^{11} \frac{\text{SF}((H_k - I_k)e^{-i\varphi_r t})}{M_s} \tag{3}$$

Equation (3) contains all the information of the sample which otherwise vague during the post processing. The angular spectrum method is used to propagate the image from the sensor plane to the sample [16]. The transfer function to control this propagation is given in Eq. (4). The ‘ λ ’ is the illumination wavelength and ‘ z ’ is the propagation distance.

$$\text{SF}(f_x, f_y) = \begin{cases} \left[\frac{2\pi i \cdot z}{\lambda} \sqrt{1 - (\lambda f_x)^2 - (\lambda f_y)^2} \right] & f_x^2 + f_y^2 \leq \frac{1}{\lambda^2} \\ 0 & \text{elsewhere} \end{cases} \tag{4}$$

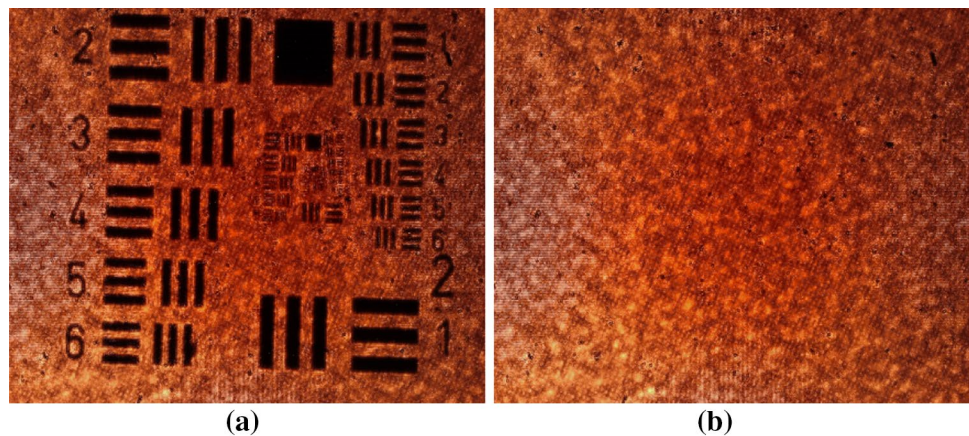
Primary condition for the experiment is the calibration of optical system, in which the images are recorded with phase mask at different axial planes without sample. The images are referred as ‘reference images’, which carry the information of the system, including the wave fronts of the illuminating source and phase of phase mask during each illumination. In Eq. (2, 3), ‘ I ’ represents the reference image while φ_r is the phase of plane waves incident on the sample. The phase of plane wave is the accumulative phase of

illuminating beam and phase mask. The out of focus scanning gathers the lost phase and amplitude information of the sample between the sample and sensor planes. To collect lost or scattered sample information the SS is moved along the axial direction and holograms are recorded at different planes. At each plane, an image is captured with different frequency contents of the sample due to diffraction effect. The parameters which contribute for diffraction are the wavelength of illumination and separation between the sample and sensor while both parameters, in our case, remain constant throughout the experimentation. The multi-height technique can also be tested while keeping the axial scanning in a random walk step instead of periodic steps within the same travel range. In both cases, the important point is the maximum limit/range of scanning which depends upon the signal–noise ratio. The minimum distance between the sample and sensor is decided from the geometry of the sensor while the ideal value should be from 200 to 500 μm . The z_2 value is measured through the autofocusing algorithm through Matlab software. The algorithm of autofocusing is simple and straightforward in which the recorded image is translated to different z -planes with roughly known range of z_2 -values. The image with highly focused result/sharp edges decide the separation of sample and sensor. The images recorded without sample in the system with the same parameters as used previously.

3 Results and discussion

The sample USAF 1951 resolution chart, is used to enumerate the resolution and field of view of lensless microscopic system. Simulation and experimental results authenticate our proposed scheme, with a room of improvement to convert into commercial equipment. In Fig. 2 only a hologram recorded at z_1 -value 8.75 cm and a diffraction pattern without sample is shown. The twin image effect is prominent in the hologram contents. The comparison of conventional

Fig. 2 **a** Recorded hologram with sample and **b** image without sample



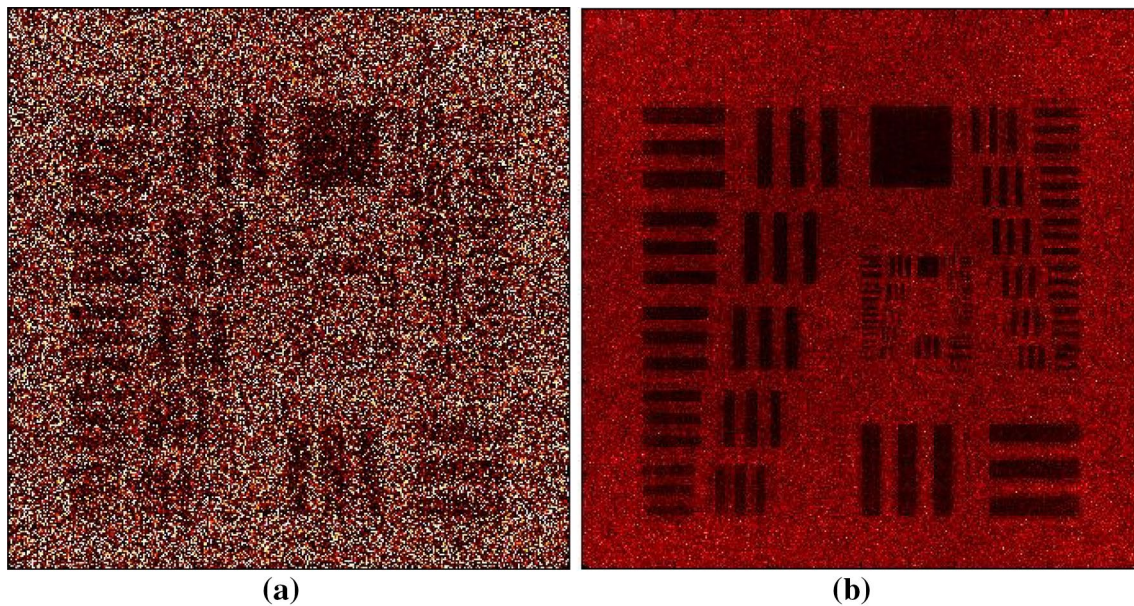
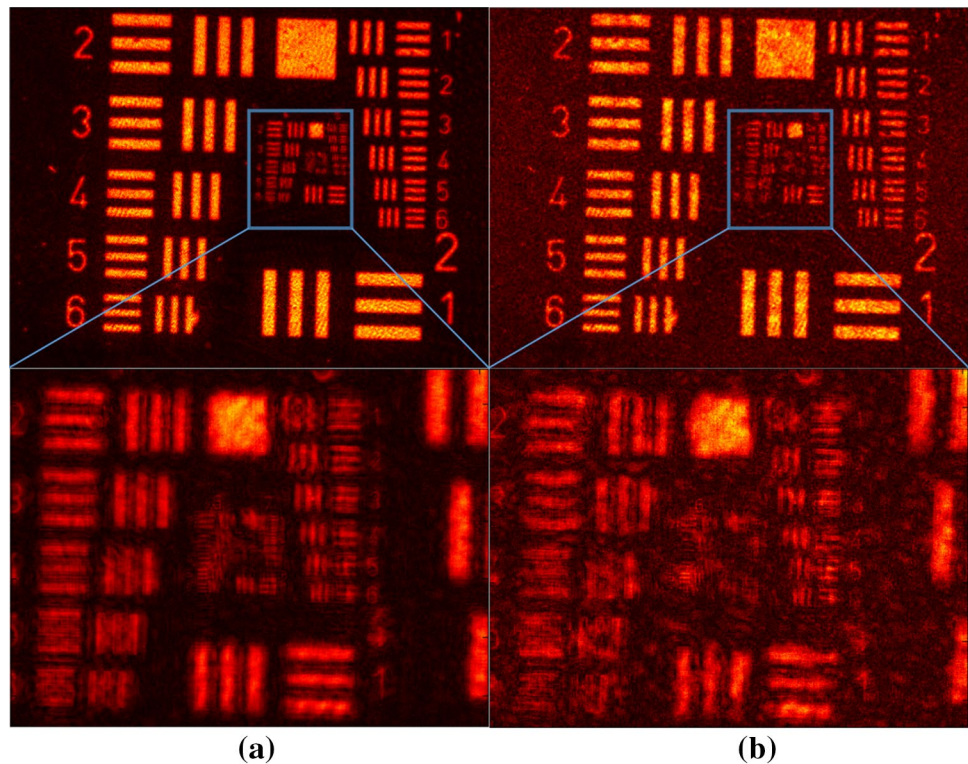


Fig. 3 Comparison of simulation result: **a** conventional image, **b** superresolved image as a result of multi-heights illumination method

image with super resolved image through axial scanning of sensor is shown in Fig. 3 for simulation results. The low signal–noise ratio (SNR) of conventional image make it blur while the SNR value is increased through axial scanning and resultant image is shown in Fig. 3b. The resolution of the final image is $1.4 \mu\text{m}$ which is almost equal to the pixel size of image sensor. The other parameters including wavelength and sample and sensor separation are adjusted according to the experimental achievable parameters. The large field of view and resolution enhancement are achieved in the simulation result. For the experimental result, similar USAF 1951 resolution chart from Edmund Optics is used to justify the proposed technique. The total number of raw images are 22, whereas 11 images are captured without sample and 11 with samples in the optical setup. The two types of images are mutually subtracted at the corresponding planes, i.e. different z_1 -planes. The resultant images are propagated to the sample plane through angular spectrum propagation method [14]. All the propagated images are added to give final image with high signal–noise ratio and improved resolution. The specification of equipment used in this experiment is coherent light source of wavelength 635 nm from Coherent Source Company and the spatial light modulator (SLM) is the phase only from Daheng Company with pixel size of $12 \mu\text{m}$. The CMOS sensor used in this experiment is from Sony with pixel size of 1.4 micron. As discussed in detail in the above section, that total 22 images are recorded in which 11 are with sample and 11 without sample. In case of without prior knowledge of sample, a single line appeared as double lines which is basically a twin image effect. In off-axis holography, the removal of twin image is relatively easy to

the on-axis holography. The experimental results shown in Fig. 4a, b are conventional image and super resolved image, respectively. The resolution of retrieved image is $\sim 4 \mu\text{m}$ which is less than the simulated value due to few experimental restrictions. The main factor which limits this value is the z_2 -value between the sample and sensor. For the sensor used in this experiment, the minimum z_2 -value is $950 \mu\text{m}$ due to manufacturing geometry of the sensor. To improve this value, special sensor for lensless microscopy is needed with active area raised above the neighboring circuits. For large z_2 -value, the phase information lost in between the two planes and never reach to the sensor plane. In other words, the exact phase retrieval depends upon the minimum z_2 -value. The second limitation come from the number of illuminations, which can be increase from 11 to large number depending upon the step size. This would improve the image resolution but on other hand would reduce the processing speed. This will be user-defined variable, and would probably decide according to their requirement. In Fig. 4, the middle portion of both images are magnified for the purpose of comparison. The central portion are the group 6 and 7 with similar pattern as for group 4 and 5. The resolution of group 6 and 7 promised the resolution limit of about 4 microns as the USAF resolution chart 1951 used in this experiment from Edmund optics (Stock No. #58198) has resolution of $\sim 4 \mu\text{m}$ for group 7.

Fig. 4 Comparison of experimental result: **a** superresolved image from same phase pattern at different heights **b** conventional image obtained with single phase mask pattern



4 Conclusion

The suggested scheme is preferred due to the compact and simplified system modality. This scheme eliminates the usage of multiple phase masks which is expansive for commercial use. Second, this scheme is based on the sensor axial scanning through motorized controller from Thorlabs, which suppresses the error addition from the mechanical motion. The final result of this scheme is the same as those results obtained from the previous work mentioned in “Introduction” section. The resolution of 4 micron and field of view of 15 mm² are the experimentally achieved values. The future recommendations for this scheme are to evaluate the multi-heights method either scanning of sensor or sample in a vertical column and fixed the phase mask correspondingly. One of the apparent difference would be the scanning step size, due to very small value of z_2 . The approximate step size would be in micron, which demands highly precise micro-controller. The technique can also be tested for the phase retrieval of bio sample. This experiment was performed to establish the resolution improvement and large field of view realization. To convert this prototype into commercial microscope, few modifications like manufacturing of new sensor are needed. Such type of techniques have numerous

applications in biomedical imaging which required compact size of system with fast imaging speed.

Acknowledgements This work is supported by the National Key Research and Development Program of China (2016YFF0101400); National Natural Science Foundation of China (6171101129, 61427818, 61827825, and 61735017).

References

1. J.W. Goodman, Introduction to fourier optics (McGraw-Hill, 1968)
2. X. Zhang, I. Khimji, U.A. Gurkan, U.A.H. Safaee, P.N. Catalano et al., *Lab Chip* **11**, 2535–2540 (2011)
3. G. Jin, I.-H. Yoo, S.P. Pack, J.-W. Yang, U.-H. Ha et al., *Biosens. Bioelectron.* **38**, 126–131 (2012)
4. L.M. Lee, X. Cui, C. Yang, *Biomed. Microdevices* **11**, 5 (2009)
5. A.F. Coskun, T.-W. Su and A. Ozcan: *Lab Chip*, 10(2010)
6. B. Khademhosseini, G. Biener, I. Sencan, A. Ozcan, *Appl. Phys. Lett.* **97**, 21 (2010)
7. I. Sencan, A.F. Coskun, U. Sikora, A. Ozcan, *Sci. Rep.* **4**, 3760 (2014)
8. T.-W. Su, S.O. Isikman, W. Bishara, D. Tseng, A. Erlinger, A. Ozcan, *Opt. Exp.* **18**, 9 (2010)
9. W. Luo, A. Greenbaum, Y. Zhang, A. Ozcan, *Light Sci. Appl.* **4**, e261 (2015)
10. W. Bishara, T.-W. Su, A.F. Coskun, A. Ozcan, *Opt. Exp.* **18**, 11 (2010)
11. G. Zheng, S.A. Lee, S. Yang, C. Yan, *Lab Chip* **10**, 22 (2010)
12. S. Bernet, W. Harm, A. Jesacher, M. Ritsch-Marte: *Opt. Exp.* **19**, 25 (2011)
13. W. Harm, C. Roeder, A. Jesacher, S. Bernet, and M. Ritsch-Marte: *Opt. Exp.* **22**, 18 (2014)
14. A. Hussain, Y. Li, D. Liu, C. Kuang, X. Liu, *Sci. Rep.* **7**, 14768 (2017)

15. A. Hussain, Y. Li, D. Liu, C. Kuang, X. Liu, J. Biomed. Opt. **22**, 11 (2017)
16. W. Luo, Y. Zhang, Z. Göröcs, A. Feizi, A. Ozcan, Sci. Rep **6**, 22738 (2016)

Publisher's Note Springer Nature remains neutral with regard to jurisdictional claims in published maps and institutional affiliations.